EFFECTIVE INFRARED EMISSIVITY OF CLOUDS IN ANTARCTICA

Sadao KAWAGUCHI

National Institute of Polar Research, 9–10, Kaga 1-chome, Itabashi-ku, Tokyo 173

Abstract: This paper presents the infrared effective emissivity value of low and middle clouds deduced from 26 radiometersonde ascents carried out during 1967–1969, at Syowa Station, East Antarctica.

The average cloud emissivities were 0.83 for the downward and 0.69 for the upward flux. The discrepancy was mainly due to the difference of the spectral distribution of both fluxes, as the downward flux over cloud top is very small in comparison with the equivalent black body radiation due to the scarcity of water vapor in the upper atmosphere in Antarctica. In this study, the effective emissivity was dominated more by the radiation field of the cloud circumference than by the radiative property of cloud itself.

The emissivity increased with increasing cloud thickness till 800–1000 m, and thereafter had a high constant value about 0.95 for the downward flux. The emissivity showed a decreasing tendency with increasing cloud base height.

The IR radiative cooling of cloud is very notable; cooling rate of some 10 degrees centigrade per day was found in the upper part of cloud, and some zero cooling rate or heating was found in the lower part.

1. Introduction

In recent years interest has been taken in the radiative properties of clouds. Such information is necessary for heat budget studies for the calculation of heating rates to be used in numerical models, and for the interpretation of radiometric data available from meteorological satellites.

There are a few individual case study reports of measured infrared cloud emissivites. KUHN (1963) obtained "effective" long-wave emissivity of clouds from the measurement by radiometersonde and aircraft, and ALLEN (1971) measured the cloud emissivity in the 8–13 μm waveband by radiometersonde. PALTRIDGE (1971, 1974a, b) presented the result of simultaneous measurements of the microphysics and the thermal radiation field of straticumulus clouds by aircraft. PLATT (1975), PALTRIDGE and PLATT (1981) investigated the microphysics and the emissivity of cirrus cloud by lidar and radiometric observation. COX (1971, 1976) deduced the mean effective infrared emissivity values of cloud in midlatitudes and the tropical zone from 300 IQSY radiometersonde ascents. PALTRIDGE and PLATT (1976) and STEPHEN *et al.* (1978) summarized the result of radiometric observation of cloud by the CSIRO Division of Atmospheric Physics.

Those studies were with the cloud in mid-latitudes and the tropical zone, and have not been done in the polar region. Radiative properties of cloud in the polar region where the atmosphere has low temperature and a small amount of water vapor would

be different from those in mid-latitudes and the tropical zone. This paper examines the radiative properties of cloud in Antarctica from radiometersonde ascents at Syowa Station (69°00'S, 39°35'E) and presents the infrared emissivity of low or middle cloud.

2. Radiometersonde Data and Analysis Technique

Radiometersonde data used in this study were obtained with the Suomi-Kuhn type sonde R-66A. The accuracy of the sonde has been investigated by the international radiometersonde intercomparison program (GILL and KUHN, 1973). Radiometersonde flights of 102 were carried out during the southern polar winters of 1967–1969 at Syowa Station, East Antarctica.

About half of all flights were under clear sky, 26 flights were under low or middle horizontal homogeneous overcast cloud, and other cases were almost under broken cloud and a few cases were under upper cloud only. One cannot infer exactly whether upper cloud existed or not in the cases of low or middle overcast cloud. The distribution of the upward and downward infrared fluxes is determined from measured air temperature, pressure and radiometer temperature. Next, one must detect cloud top and base. It is not so difficult in the case of low or middle overcast cloud, but very difficult in the case of brocken cloud, so 26 cases of low and middle overcast cloud were treated in this study.

KUHN (1963) had shown that the changes of slopes of the upward and downward fluxes as a function of height might be used to detect the cloud top and base. Humidity profile gained from radiosonde data was also refered to cloud detection.

Following KUHN (1963) and COX (1971) the effective emissivity can be defined.

$$F_b\downarrow = F_t\downarrow(1-\varepsilon\downarrow)+\varepsilon\downarrow\sigma T_b^4 ,$$

so

$$\varepsilon\downarrow = \frac{F_b\downarrow - F_t\downarrow}{\sigma T_b^4 - F_t\downarrow} , \tag{1}$$

for the downward flux, and

$$F_t\uparrow = F_b\uparrow(1-\varepsilon\uparrow)+\varepsilon\uparrow\sigma T_t^4 ,$$

so

$$\varepsilon\uparrow = \frac{F_b\uparrow - F_t\uparrow}{F_b\uparrow - \sigma T_t^4} , \tag{2}$$

for the upward flux.

In eqs. (1) and (2), $F\uparrow$ and $F\downarrow$ refer to the upward and downward measured infrared fluxes respectively. The subscripts t and b refer to the top and base of the cloud layer, and σ is the Stefan-Boltzman constant. Effective emissivities for the upward and downward fluxes are different in general, because the spectral distribution of the two fluxes is quite different.

3. Results

Figure 1 shows the upward and downward measured infrared fluxes and the net

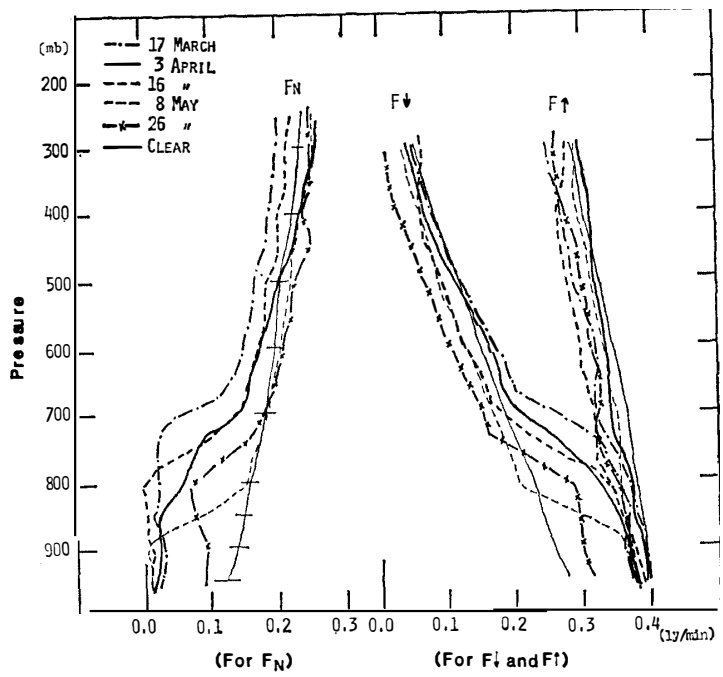

Fig. 1. The upward and downward measured infrared radiation fluxes and the net infrared radiation fluxes in early winter, at Syowa Station.

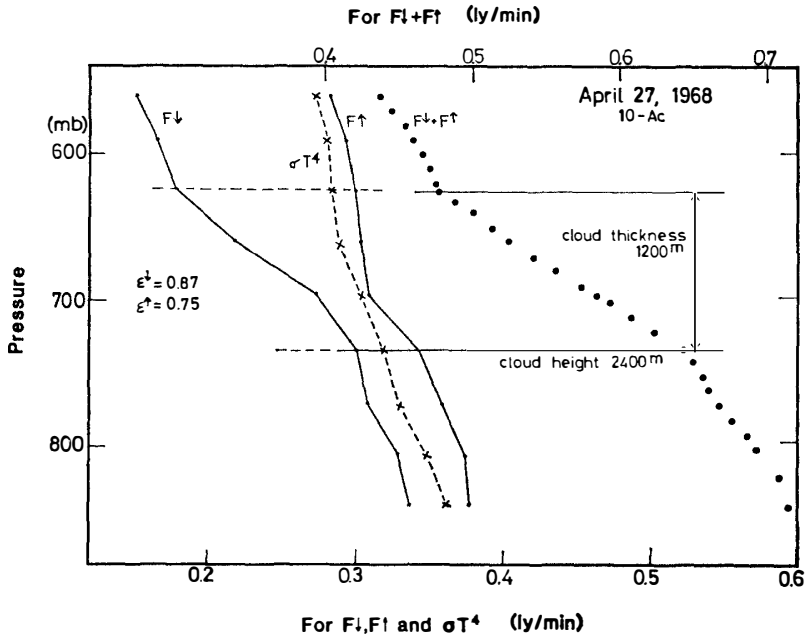

Fig. 2. Example of analysis following KUHN, the case of altocumulus cloud, equivalent radiation σT^4, downward and upward infrared radiation flux $F\downarrow$, $F\uparrow$.

infrared flux (F_N) in early winter. Thin lines show the average value of 10 cases of clear sky, and the short thin horizontal lines crossing the thin line for F_N indicate the standard deviation around the averaged F_N value. The slopes of $F\uparrow$ are not so different between the clear and cloud cases, but the slopes of $F\downarrow$ show a very large differ-

ence, the lines for $F\downarrow$ of cloudy case have very distinct bends which point out the cloud top and base.

Figure 2 shows the example of analysis following KUHN (1963). The ordinate is pressure on a linear scale and the bottom abscissa is for $F\downarrow$, $F\uparrow$ and σT^4 that is the equivalent black body radiation flux for the air temperature, the top abscissa is for $F\downarrow+F\uparrow$. The cloud top is distinct by the abrupt change of the slope of $F\downarrow$, but the cloud base is not so clear on the slopes of $F\downarrow$ and $F\uparrow$. The slope of $F\downarrow+F\uparrow$ compensates for this, the cloud base at a height of 2400 m becomes clear on the slope of $F\downarrow+F\uparrow$. In this case, the effective emissivities of altocumulus cloud layer are 0.87 and 0.75 for $\varepsilon\downarrow$ and $\varepsilon\uparrow$ respectively.

Figures 3 and 4 illustrate the cases of observed 10/10 altostratus cloud layer on March 17, 1967 and 9/10 stratocumulus cloud layer on June 30, 1967. Air tem-

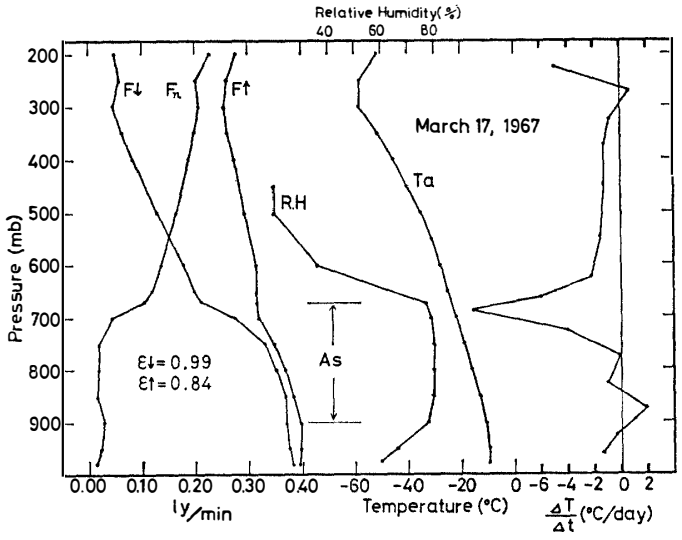

Fig. 3. Profiles of downward, upward and net infrared radiation fluxes and air temperature Ta, relative humidity R.H radiation cooling rate, for the case of altostratus.

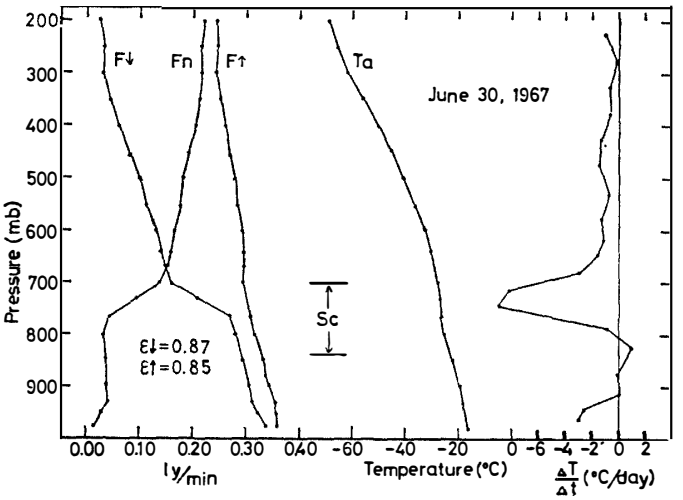

Fig. 4. Same as Fig. 3 but for the case of stratocumulus.

perature, relative humidity (Fig. 3 only) and the cooling rate expected from flux divergence are shown with downward, upward and net infrared radiative fluxes. The top abscissa is relative humidity and the bottom abscissa has three scales, one for radiative flux in langleys per minute, one for temperature in degrees Celsius and the other for cooling rate in degrees Celsius per day.

In Fig. 3, the cloud top is obvious on the slopes of $F\downarrow$ and of the relative humidity, and the cloud base is also obvious on the slopes of $F\uparrow$ and of the relative humidity. The cloud thickness was 1900 m, and the cloud base was at some 700 m height. The effective emissivities of this cloud are 0.99 and 0.84 for $\varepsilon\downarrow$ and $\varepsilon\uparrow$ respectively. The infrared radiative cooling is very notable, cooling rate of some 12 degrees per day is found in the upper part of the cloud, and near zero cooling rate or heating is found in the lower part.

Figure 4 shows the case of stratocumulus cloud whose frequency of appearance is very high in the Antarctic coast region. The cloud top is obvious, but the cloud base is obscure on the slope of the downward flux, the weak change of the slope of the upward flux point out the cloud base, the slope of $F\downarrow+F\uparrow$ will make it more clear. The effective emissivities are 0.87 for $\varepsilon\downarrow$ and 0.85 for $\varepsilon\uparrow$. The IR cooling rate is very notable also in this case, cooling rate of some 9 degrees per day in the upper part of the cloud and heating rate of one degree in the lower part are found.

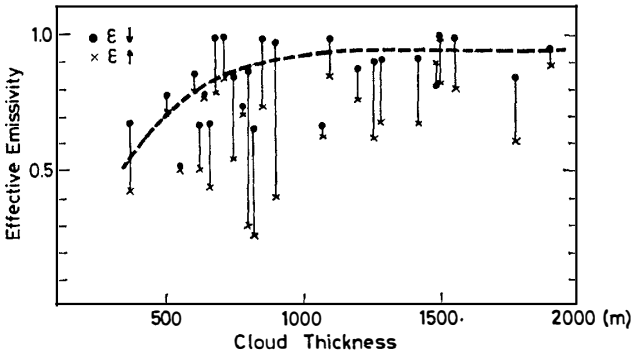

Fig. 5. Cloud emissivity as a function of cloud thickness. Emissivity for downward flux $\varepsilon\downarrow$ and upward flux $\varepsilon\uparrow$ in the same case is connected by solid line. Dashed curve shows the trend of the emissivity for downward flux $\varepsilon\downarrow$.

The effective emissivities of 26 cases have been plotted in Fig. 5 in which the ordinate is effective emissivity and the abscissa is cloud thickness, $\varepsilon\downarrow$ and $\varepsilon\uparrow$ of the same cloud are connected by the solid line. The emissivity for downward flux $\varepsilon\uparrow$ is larger than that of upward flux $\varepsilon\uparrow$ except only one case, and the averaged values of $\varepsilon\downarrow$ and $\varepsilon\uparrow$ are 0.83 and 0.69, and the ranges are from 0.5 to 1.0 and from 0.25 to 0.98 respectively.

The emissivity for the downward flux becomes large with the increase of the cloud thickness, and ranges from 0.8 to 1.0 in the cloud thickness of more than 800 m, the dashed curve shows the trend of the emissivity for the downward flux as a function of cloud thickness. The emissivity of the upward flux becomes also large with the increase of the cloud thickness, and ranges from 0.6 to near 1.0 for the cloud thickness of more than 1000 m.

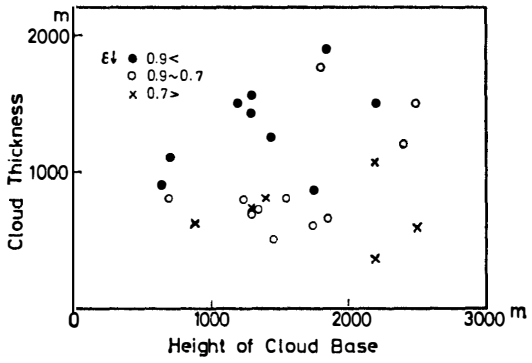

Fig. 6. Cloud emissivity for downward flux $\varepsilon\downarrow$ as a function of cloud thickness and of cloud height.

The emissivities for downward flux $\varepsilon\downarrow$ are plotted as a function of cloud thickness and height of cloud base in Fig. 6. Although the relation of the emissivity and the height of cloud base is not so distinct, one can find a tendency of the decrease of the emissivity with the increase of the cloud base height.

4. Discussion and Concluding Remarks

The discrepancy between $\varepsilon\downarrow$ and $\varepsilon\uparrow$ is large, which is mainly due to the difference between the spectral distribution of the downward flux at the cloud top $F_t\downarrow$ and of the upward flux at the cloud base $F_b\uparrow$. In comparison with the black body radiation of equivalent temperature, the downward flux $F\downarrow$ over the cloud is very small, due to the scarcity of water vapor in the upper atmosphere. The window region occupies about 30% of the radiative energy of the equivalent black body at minus 30 degree that was the mean temperature of the cloud top in 26 cases. Under the sufficient water vapor content over the cloud top, $F_t\downarrow/\sigma T_t^4$ could be 0.7 or more. PALTRIDGE (1971) obtained the value of 0.8 in the tropical zone, and FEIGEL'SON (1973) showed the value from 0.7 to 0.8, but the value obtained in this experiment was only 0.61. The spectral energy of $F\downarrow$ could not be saturated also in outside the window region. The property of $F_t\downarrow$ caused the abrupt change of the downward flux in the upper part of the cloud, and as a result, the difference between $F_t\downarrow$ and $F_b\downarrow$ is large, and the emissivity for the downward flux becomes large following eq. (1). The small $F_t\downarrow$ is also one of the causes for the large infrared cooling rate in the upper part of the cloud.

On the other hand, the difference between σT_b^4 and $F_b\uparrow$ that can be determind by the ground surface temperature close to T_b and by the temperature of the atmosphere containing comparatively much water vapor under the cloud base, is small. So the change of the slope of $F\uparrow$ in the cloud is gradual, and it could show the radiative property of the cloud in itself.

As stated above, the effective emissivity and the infrared cooling of cloud are dominated not only by the radiative property of cloud itself, but also by the radiation field of the circumference of the cloud.

Acknowledgments

The author would like to express his thanks to Prof. M. TANAKA, Upper Atmosphere Research Laboratory of Tohoku University, for his helpful discussions. He is also indebted to members of the meteorological observation of the wintering party of Japanese Antarctic Research Expedition for obtaining data. He wishes to express his thanks to Ms. K. SUKENO for her assistance in preparing the manuscript.

References

ALLEN, J. R. (1971): Measurements of cloud emissivity in the 8–13 μ waveband. J. Appl. Meteorol., **10**, 260–265.

COX, S. K. (1971): Cirrus clouds and climate. J. Atmos. Sci., **28**, 1513–1515.

COX, S. K. (1976): Observations of cloud infrared effective emissivity. J. Atmos. Sci., **33**, 287–289.

FEIGEL'SON, E. M. (1973): Radiant Heat Transfer in a Cloudy Atmosphere. Tr. by D. LEDERMAN from Russian. Jerusalem, IPST, 191 p.

GILL, J. C. and KUHN, P. M. (1973): The International Radiometersonde Intercomparison Programme (1970–1971). Geneva, WMO, 127 p. (WMO Tech. Note, **128**).

KUHN, P. M. (1963): Measured effective long-wave emissivity of clouds. Mon. Weather Rev., **91**, 635–640.

PALTRIDGE, G. W. (1971): Solar and thermal radiation flux measurements over the east coast of Australia. J. Geophys. Res., **76**, 2857–2864.

PALTRIDGE, G. W. (1974a): Infrared emissivity, shortwave albedo and the microphysics of stratiform water clouds. J. Geophys. Res., **79**, 4053–4059.

PALTRIDGE, G. W. (1974b): Atmospheric radiation and the gross character of stratiform cloud. J. Atmos. Sci., **31**, 244–250.

PALTRIDGE, G. W. and PLATT, C. M. R. (1976): Radiative Processes in Meteorology and Climatology. Amsterdam, Elsevier, 318 p. (Developments in Atmospheric Science, **5**).

PALTRIDGE, G. W. and PLATT, C. M. R. (1981): Aircraft measurements of solar and infrared radiation and the microphysics of cirrus cloud. Q. J. R. Meteorol. Soc., **107**, 367–380.

PALTRIDGE, G. W. and SARGENT, S. L. (1971): Solar and thermal radiation measurements to 32 km at low solar elevations. J. Atmos. Sci., **28**, 242–253.

PLATT, C. M. R. (1975): Infrared emissivity of cirrus-simultaneous satellite, lider and radiometric observations. Q. J. R. Meteorol. Soc., **101**, 119–126.

STEPHENS, G. L., PALTRIDGE, G. W. and PLATT, C. M. R. (1978): Radiation profiles in extended water clouds. III: Observations. J. Atmos. Sci., **35**, 2133–2141.

(Received April 30, 1983; Revised manuscript received June 17, 1983)